Parallel genetic adaptation of *Bacillus subtilis* to different plant species

Guohai Hu[1,2,3,7], Yue Wang[1,2,4,7], Christopher Blake[3], Mathilde Nordgaard[3], Xin Liu[1,2,4], Bo Wang[1,2,5,*], Ákos T. Kovács[3,6*]

[1] China National GeneBank, BGI-Shenzhen, 518120 Shenzhen, China

[2] BGI-Shenzhen, 518083 Shenzhen, China

[3] Bacterial Interactions and Evolution Group, DTU Bioengineering, Technical University of Denmark, 2800 Lyngby, Denmark

[4] BGI-Beijing, Beijing, 102601, China

[5] Shenzhen Key Laboratory of Environmental Microbial Genomics and Application, BGI-Shenzhen, 518083 Shenzhen, China

[6] Institute of Biology Leiden, Leiden University, 2333BE Leiden, The Netherlands

[7] These authors contributed equally

[*]Corresponding authors: a.t.kovacs@biology.leidenuniv.nl (Ákos T. Kovács), wangbo@cngb.org (Bo Wang)

Guohai Hu	huguohai@cngb.org	https://orcid.org/0000-0003-2756-8328
Yue Wang	wangyue2@genomics.cn	https://orcid.org/0000-0003-2103-4237
Christopher Blake	christopher.blake@monash.edu	https://orcid.org/0000-0002-6904-4074
Mathilde Nordgaard	mathilde@agrobiomics.bio	https://orcid.org/0000-0003-0648-8978
Xin Liu	liuxin@genomics.cn	https://orcid.org/0000-0003-3256-2940
Bo Wang	wangbo@cngb.org	https://orcid.org/0000-0002-8657-5897
Ákos T. Kovács	a.t.kovacs@biology.leidenuniv.nl	https://orcid.org/0000-0002-4465-1636

Abstract

Plant growth-promoting rhizobacteria benefit plants by stimulating their growth or protecting them against phytopathogens. Rhizobacteria must colonise and persist on plant roots to exert their benefits. However, little is known regarding the processes by which rhizobacteria adapt to different plant species, or behave under alternating host plant regimes. Here, we used experimental evolution and whole-population whole-genome sequencing to analyse how *Bacillus subtilis* evolves on *Arabidopsis thaliana* and tomato seedlings, and under an alternating host plant regime, in a static hydroponic setup. We observed parallel evolution across multiple levels of biological organisation in all conditions, which was greatest for the two heterogeneous, multi-resource spatially-structured environments at the genetic level. Species-specific adaptation at the genetic level was also observed, possibly caused by the selection stress imposed by different host plants. Furthermore, a trade-off between motility and biofilm development was supported by mutational changes in motility- and biofilm-related genes. Finally, we identified several condition-specific and common targeted genes in different environments by comparing three different *B. subtilis* biofilm adaptation settings. The results demonstrate a common evolutionary pattern when *B. subtilis* is adapting to the plant rhizosphere in similar conditions, and reveal differences in genetic mechanisms between different host plants. These findings will likely support strain improvements for sustainable agriculture.

Key words: adaptation, experimental evolution, plant-bacteria interaction, trade-off, *Bacillus subtilis*

Data summary

Sequencing data associated with this article are available in the CNGB Sequence Archive (CNSA) [1] of the China National GeneBank DataBase (CNGBdb) [2] under accession numbers CNP0002416 and CNP0003952. Strain data for the DK1042 ancestor are available under accession number CNP0002416.

Impact statement

For rhizobacteria to benefit plant growth and protect against phytopathogens, bacteria must colonise and persist on plant roots. Understanding how rhizobacteria adapt to different plant species will assist strain development in sustainable agriculture. To explore the rhizobacterial adaptation process for different plant species and alternating host regimes, *B. subtilis* was experimentally evolved on *A. thaliana* or tomato roots, or an alternating host regime. Both parallel and species-specific adaptation was revealed at the genetic level. Analysis of the trade-off between motility and biofilm formation revealed several condition-specific and commonly targeted genes based on experimentally evolving *B. subtilis* biofilms.

61 # Introduction

62 In natural environments, plant growth and yield depend on a plethora of interactions within the
63 complex and dynamic communities of bacteria and fungi [3]. The rhizosphere provides a niche
64 for the mutualistic relationships between plants and microorganisms in the surrounding soil.
65 Plants exude up to 20% of fixed carbon and 15% of nitrogen into their environment [4, 5], and
66 these exudates shape the microbiome. Importantly, the amount and composition of exudates
67 vary depending on plant species, stage of development and environmental stresses [6]. Exudates
68 contribute to rhizobiome formation by recruiting plant growth-promoting rhizobacteria (PGPR)
69 and serving as nutrients [7], and PGPR benefit plant growth and enhance plant tolerance to
70 different abiotic and biotic stresses [8]. *Bacillus subtilis* is a soil-dwelling, biofilm-forming
71 Gram-positive PGPR commonly found in association with plants and their rhizosphere [9]. This
72 bacterial species aids plants in several direct and indirect ways [10]. Some *B. subtilis* strains
73 have been applied as biocontrol agents within agriculture, but the effects vary immensely under
74 field conditions [11, 12]. To exert their beneficial effects, PGPR must colonise and persist on
75 the root surface, which mainly depends on their ability to form biofilms.

76 Each plant species has a distinct effect on its rhizobiome and this is partly driven by plant-
77 secreted exudates. Root exudates not only provide a nutritional source for soil microorganisms,
78 but also serve as a signal to attract or repel specific groups of microbes [13]. For example,
79 diverse sugars and organic acids induce biofilm formation of *B. subtilis in vitro* or directly on
80 the plant via different molecular mechanisms. Spo0A is a central transcriptional regulator in *B.*
81 *subtilis* involved in biofilm development [14]. Biofilm formation is triggered when moderate

82 levels of phosphorylated Spo0A (Spo0A-P) are present within a cell. The level of Spo0A-P is
83 controlled by five histidine kinases (KinA–E), which respond to different environmental signals
84 [15]. Chen and colleagues found that *B. subtilis* biofilm formation on tomato roots is dependent
85 on KinD and small signalling molecules, possibly L-malic acid, released by the roots to
86 stimulate *B. subtilis* biofilm *in vitro* [16]. Unlike in tomato, deletion of *kinCD* has only a
87 moderate effect on biofilm formation on *Arabidopsis thaliana* roots [17], suggesting that the
88 kinase requirement of *B. subtilis* for root colonisation varies between plant species. In the case
89 of *A. thaliana*, biofilm formation by *B. subtilis* is triggered by plant polysaccharides pectin,
90 arabinogalactan and xylan, which act both as environmental cues and substrates for matrix
91 synthesis [17]. Moreover, the disaccharide sucrose that is abundantly secreted from plant roots
92 activates a signalling cascade to trigger solid surface motility and promote rhizosphere
93 colonisation by *B. subtilis* [18].

94 Interestingly, a *B. subtilis* strain isolated from banana rhizosphere and a *Bacillus*
95 *amylolicefaciens* strain isolated from cucumber rhizosphere colonise their original plant hosts
96 more efficiently than the non-host plant [19], demonstrating species-specific colonisation.
97 Additionally, organic acids detected exclusively in one plant species induce chemotaxis and
98 biofilm formation of the corresponding bacterial isolate from that given host [19]. Chemotaxis
99 and swarming motility are important for plant colonisation [19, 20]; when defective in either,
100 the ability of *B. subtilis* to efficiently colonise tomato seedlings was reduced in a gnotobiotic
101 system [20]. Similarly, mutants lacking flagellum production were unable to colonise the roots
102 of *A. thaliana* in a static hydroponic setup and tomato in a gnotobiotic system [20, 21].

103 In addition to testing specific mutants, experimental evolution provides a powerful tool for
104 revealing the molecular mechanisms related to plant interactions because microbes adapt to the
105 plant root niche [22]. Experimentally evolved clones of *Bacillus thuringiensis* from *A. thaliana*
106 roots displayed improved root colonisation ability and enhanced swarming, but impaired
107 swimming, in addition to altered bacterial differentiation and pathogenicity [23]. In a similar
108 setup, when *B. subtilis* was adapted to *A. thaliana* roots, evolved isolates demonstrated elevated
109 root colonisation and impaired swimming and swarming motility [24], indicating a possible
110 biofilm-motility trade-off. *Pseudomonas protegens*, adapted to *A. thaliana* rhizosphere under
111 axenic sandy conditions, exhibited enhanced swimming motility and impaired swarming
112 motility [25]. Although these results highlight the existence of an evolutionary trade-off
113 between biofilm development and motility, it remains largely unknown how such mechanisms
114 supervene from an evolutionary perspective.

115 Since crop rotation regime has great influence on soil multifunctionality and bacterial
116 community in agroecosystems [26], we wondered whether a plant-colonising bacterium adapts
117 differently in an alternating host regime compared with using the same plant throughout the
118 experiment. In addition, we questioned what portion of bacterial adaptation on a plant root will
119 be host-specific. To explore these questions, we employed experimental evolution combined
120 with whole-population metagenome sequencing to analyse how *B. subtilis* evolves on *A.*
121 *thaliana* and tomato seedlings, as well as in an alternating host regime of these two species in
122 a static hydroponic setup. We observed parallel evolution across multiple levels of biological
123 organisation and a higher gene-level parallelism in populations evolved in an alternating host

124 regime. We also observed species-specific adaptation at the genetic level, which was potentially
125 provoked by specific host plant-imposed selection, either due to root exudates, plant
126 polysaccharides, or certain stress conditions. Additionally, motility-biofilm trade-off was
127 revealed in the mutational landscape of related genes, in addition to reduced swimming and
128 swarming motility. Finally, we identified several condition-specific and shared mutated genes
129 of *B. subtilis* when evolved in different biofilm environments.

Methods

Bacterial strains and experimental methods

We used identical materials and methods for tomato and two host-cycling evolution setups as described previously for the *A. thaliana* selection approach [27], including the bacterial strain and culture conditions, seedling preparation, experimental evolution, and morphological diversification experiments.

Experimental evolution

To initiate experimental evolution we used *A. thaliana* Col-0 seedlings at 14–16 days old and tomato Col-0 seedlings at 8–10 days old. Seedlings were placed in 100 ml reagent bottles containing 27 ml of MSNg and inoculated with 3 ml of *B. subtilis* DK1042 bacterial culture adjusted to $OD_{600} = 0.2$, resulting in a starting OD_{600} of 0.02. To ensure that roots but not sprouts or leaves provided surface for colonisation, seedlings were pulled through a sterile nylon mesh floating on top of the liquid medium, leaving only the roots submerged in the medium. Seedlings were incubated for 48 h under static conditions in a plant chamber with a day/night cycle of 16 h light at 24°C and 8 h dark at 20°C. We conducted two mono-host evolution experiments, one using only ***A***. *thaliana* (Bs_root_**A**) and another with **T**omato (Bs_root_**T**), as well as two host-cycling evolution experiments, which either started on ***A***. *thaliana* (Bs_root_**A**T) or **T**omato (Bs_root_**T**A) and switched plant species after every third transfer. Therefore, four different evolution experiments each with five parallel lineages (A to E) were passaged on both *A. thaliana* and tomato seedlings for 20 transfers, spanning 40 days (**Fig. 1a**

and **1b**). Consequently, every 2 days, a previously colonised plant seedling was transferred to a new sterile seedling, allowing only bacterial cells attached to the new root to continue in the experiment, enabling selection for a continuous cycle of dispersal, chemotaxis towards the plant root and biofilm formation on the root. To keep track and ensure sterile handling of seedlings during evolution, two controls without initial inoculant were included, in which either sterile seedlings or 10% of the MSNg medium were passaged. To follow the development of populations and test for contamination, bacterial cells colonising old roots, as well as the two controls, were plated on lysogeny broth (LB, Lennox; Carl Roth, Karlsruhe, Germany; 10 g/L tryptone, 5 g/L yeast extract, 5 g/L NaCl) agar medium after initial colonisation and after transfer 5, 10, 17 and 20.

CFU quantification

In order to isolate biofilms from seedlings for quantification, roots were detached from sprouts, carefully washed in sterile MilliQ water and vortexed vigorously for 3 min in 1 ml of 0.9% NaCl in the presence of small glass beads (Ø0.75−1.00 mm; Carl Roth, Karlsruhe, Germany). The resulting cell suspensions were plated for colony-forming units (CFU) quantification and preserved as frozen stocks for subsequent comparison and DNA sequencing.

Motility assays

A 20 mL volume of either 0.3% or 0.7% lysogeny broth (LB)-agar plates was used to test swimming and swarming motility. In both cases, plates were dried for 20 min before bacterial cultures were applied to the centre of plates. A 2 µL volume of overnight culture of ancestor or

evolved isolates adjusted to an OD_{600} of 5.0 were spotted in the middle of the plate. To maintain similar humidity across all plates, multiple stacking was avoided. Plates were incubated at 30°C and images were taken for swimming (after 6, 8 and 24 h) and swarming (after 8 , 10 and 24 h) using a Lumix DC T290 camera (Panasonic) equipped with a DC Vario-ELMAR lens (Leica). The area covered by bacterial cells at a given timepoint as well as the area of the whole agar plate were measured using Fiji ImageJ 1.52p. The capacity for swimming and swarming motility was calculated by dividing the covered area by the total area.

Sequencing and variant calling

Archived samples from each experimental evolution environment were revived via cultivation in LB medium at 37°C for 16 h. Genomic DNA was extracted from harvested cells of each culture using a EURx Bacterial and Yeast Genomic DNA Kit (EURx, Gdansk, Poland).

For whole-population genome sequencing of the evolved populations and ancestor strain samples, an MGIEasy PCR-free Library Prep Set (MGI Tech, Shenzhen, China) was used for library preparation, and 150 bp × 2 pair-end sequencing was performed on a DNBSEQ-Tx sequencer (MGI Tech) following the manufacturer's procedures [28, 29]. More than 200× depth coverage of raw data was achieved for all population samples for further polymorphism calling.

To remove low-quality data, filtering was performed using SOAPnuke (version 1.5.6) [30]. Therefore, reads including >50% of bases with quality score <12, reads including >10% of unknown bases (N) and reads containing adaptor contamination were removed. Clean data were normalised to 200× depth for all sample to ensure similar variant calling sensitivity. Mutations

were identified using *breseq* (version 0.35.7) with default parameters and a -p option for population samples [31, 32]. The default parameters reported mutations only if they included at least two reads from each strand and reached a frequency of at least 5% in the population. Mutations also present in ancestor strains were removed for further analysis.

Genotype inferences from populations and Muller plots

To generate muller plots, the *Lolipop* (version 0.6) package (https://github.com/cdeitrick/lolipop) was used with default parameters [33, 34]. These methods predict genotypes and lineages based on the shared trajectories of mutations over time to test their probability of nonrandom genetic linkage. Muller plots were then manually coloured by the presence of shared mutated genes or genotypes. Genotypes and their frequencies were used for genotype diversity calculation in R (version 4.2.2) using the vegan (version 2.6-4) package.

Jaccard Index calculation

Jaccard Index (*J*) for a pair of evolved lineages was calculated using formula (1). For a pair of lineages, each contains mutated gene set G1 and G2, respectively. In words, *J* is the number of genes mutated in both lineages divided by the total number of genes mutated in lineage 1 or lineage 2. *J* ranges from 0 to 1, with 1 indicating two lineages sharing exactly the same set of mutated genes and 0 indicating no mutated genes shared in the two lineages. This value was calculated for all pairs of evolved lineages, both within and between evolved environments.

$$J_{G1,G2} = \frac{|G1 \cap G2|}{|G1 \cup G2|} \quad (1)$$

Results

B. subtilis showed rapid improvement and diversification during evolution on plant roots

We wondered whether plant-colonising bacteria adapt differently in an alternating host regime compared with a setup in which the same plant is used throughout the experiment. To investigate this, we explored adaptation of *B. subtilis* on the roots of two different plant species and compared the results with those of an experiment in which plant hosts were sequentially alternated. Evolved clones from the Bs_root_A setup have been examined in detail previously [27]. To evaluate the improvements in root colonisation during experimental evolution, CFU per gram of roots was measured after transfer 1, 5, 10, 17 and 20 (T1, T5, T10, T17 and T20, respectively). As expected [23, 24, 27], root colonisation ability improved significantly in all evolving lineages and conditions, by an average of 9.10-fold, 7.41-fold, 25.29-fold and 11.98-fold after 20 transfers in Bs_root_A, Bs_root_T, Bs_root_AT and Bs_root_TA, respectively (**Fig. 1c**). Furthermore, morphological diversification was also observed in all evolving lineages and conditions in CFU assays with morphotypes termed as Wrinkle (WR), Snow (SN) and Smooth (SM) [27], with colony morphology of the WR variant comparable to that of the ancestor. To investigate how the distribution of the distinct morphotypes developed during experimental evolution, overnight-grown cultures of frozen stocks of evolved populations from root 5, 10, 17 and 20 as well as from the ancestral strain (transfer 0) were prepared and plated on LB-agar. Different morphological variants were identified and counted to calculate the ratio of a given morphotype at each timepoint for each lineage. In all four conditions, WR was the most abundant in all lineages throughout the experiment (**Fig. 1d**). SN appeared in all lineages

at T5, reaching an average frequency of 21.78%, 15.48%, 23.81% and 21.28% in Bs_root_A, Bs_root_T, Bs_root_AT and Bs_root_TA, respectively (**Fig. 1d**), but it was below the detection limit in some lineages at T10 and T17, then raised again in all lineages at T20. SM was observable in 11 of 20 lineages at T10 and only absent in one lineage at T17 and T20 (**Fig. 1d**). The three distinct morphotypes coexisted until the end of the evolution experiment, reaching average highly similar ratios of ~80% WR, 17% SN and 3% SM in all four evolution experiments, revealing an astounding degree of parallelism at the morphotypic level.

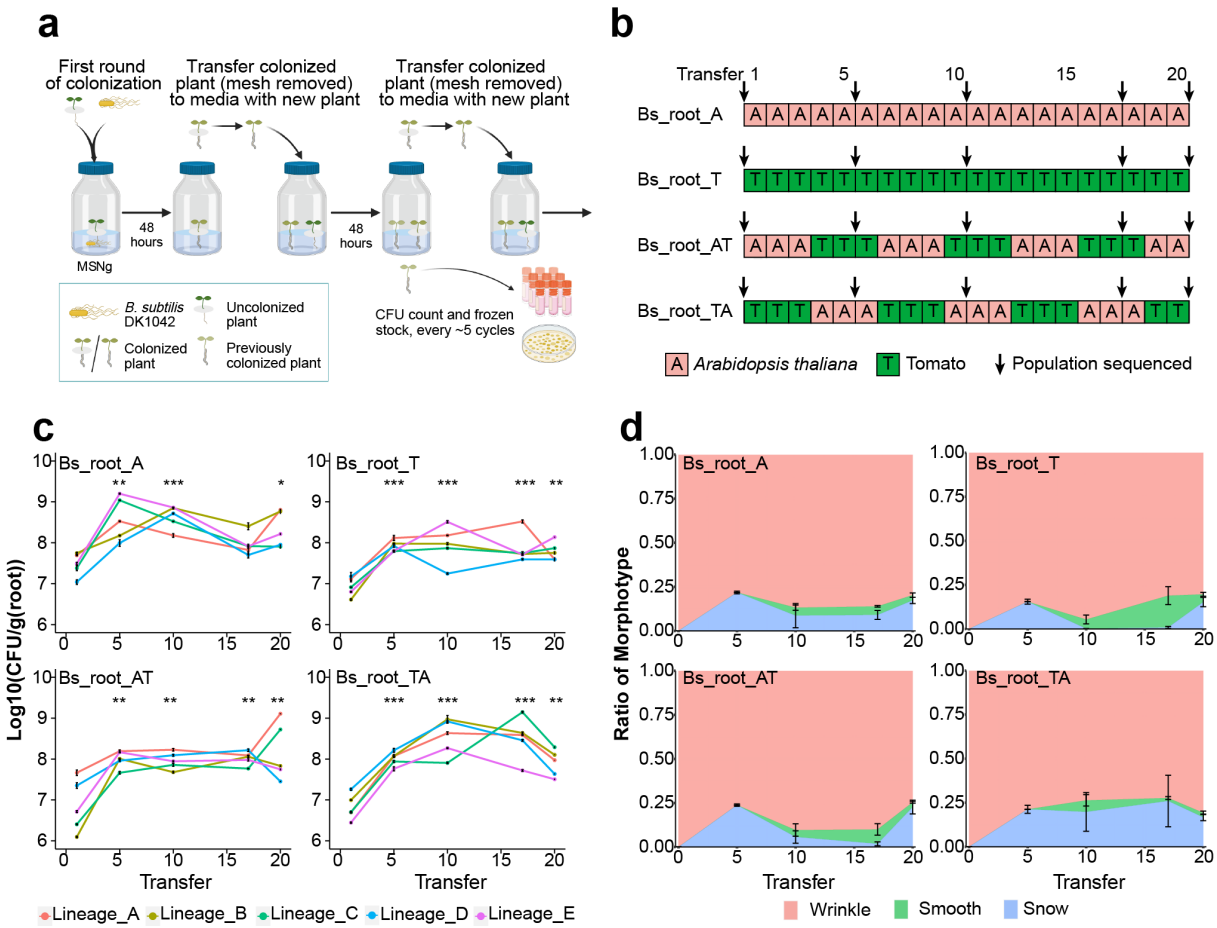

Fig. 1 Evolution of *B. subtilis* on different plant roots. a. Experimental evolution scheme of *B. subtilis* adapting to plant seedlings (created with BioRender.com), **b.** Four evolution

experiments were conducted, either as mono-evolution experiments with only *A. thaliana* or tomato seedlings, or cycling evolution experiments with plant species switched after every third transfer. Sequenced population samples are indicated by arrows. **c.** Root colonisation ability was measured as CFU per gram of root for T1, T5, T10, T17 and T20 in all lineages (n = 3, *p <0.05, **p <0.01, ***p <0.001). **d.** Dynamic frequency changes of different morphotypes in the evolution experiment averaged for all five populations in each condition (n = 5). Results are means and error bars represent standard error in **c** and **d**.

Evolved isolates showed impaired motility

In a soil environment, bacterial cells must actively move towards plant roots during the initial phase of root colonisation, as well as when recolonising [21]. We hypothesised that, in the static hydroponic setup, which selects for regular root recolonisation including chemotaxis, biofilm formation and dispersal, motility would improve significantly during the evolution experiment, resulting in better root colonisation. To examine this, evolved end-point isolates from Bs_root_A and Bs_root_T were tested for swimming and swarming motility by spotting 2µL of an overnight culture on 0.3% and 0.7% LB-agar, respectively. Contrary to our expectations, none of the seven tested isolates evolved on *A. thaliana* or the five tested isolates evolved on tomato showed improvements in either swimming or swarming (**Fig. 2**). Instead, most isolates displayed a significantly smaller swimming radius after 6 h and 8 h compared with the ancestor, although all isolates colonised the entire plate after 24 h, thus mobility was preserved. Importantly, other forms of motility such as sliding [35, 36] might mask the effect of swimming

after 24 h. Moreover, all isolates exhibited either delayed, reduced or even impaired swarming abilities. In future experiments, the frequencies of altered motility phenotype need to be assayed for each condition to clearly conclude selection against motility trait.

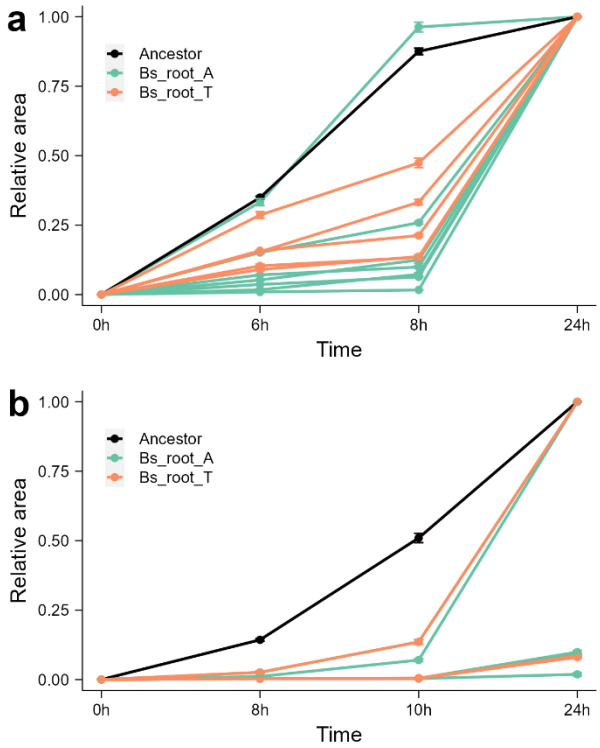

Fig. 2 Evolved isolates showed impaired motility. Swimming (a) and **Swarming (b)** motility of evolved isolates from Bs_root_A (lime green, seven isolates) and Bs_root_T (Soft orange, five isolates) compared with the ancestor (**Black**). Notably, swarming motility of several isolates were similar and low, and hence indistinguishable from each other in panel b. Results are means and error bars represent standard error, each isolate was tested in triplicate, and the ancestor was repeated 9 times. Tested isolates included two SN from lineage A and E of Bs_root_A, two SM from lineage A and E of Bs_root_A, three WR from lineage A, D and E of Bs_root_A, and five WR from lineage A (1), B (2) and C (2) of Bs_root_T.

Mutation spectrum and genetic diversity

Mutations provide the ultimate source of diversity, allowing selection to act and evolution to take place. To understand the genetic basis underlying the observed phenotypic diversification, impaired motility, and the dynamic landscape of evolution, we performed longitudinal whole-population genome sequencing of 79 *B. subtilis* population samples (one population sample was lost during freezer maintenance) and the ancestor strain, using the DNBSEQ-Tx platform [28, 29]. More than 200× coverage depth of raw data was achieved for each sample. Mutations, including single-nucleotide polymorphisms (SNPs) and short insertions and deletions (indels) were identified using the *breseq* pipeline (version 0.35.7) [31, 32]. The default parameters identified mutations only if they appeared in at least two reads from each strand and reached a frequency of at least 5% in the population. This analysis revealed 117, 106, 104 and 134 mutations in the evolved lineages from the Bs_root_A, Bs_root_T, Bs_root_AT and Bs_root_TA conditions, respectively (

Table 1). No significant difference in mutation numbers were identified between the evolution conditions (Kruskal-Wallis test, $p = 0.1277$), though the mutation spectra were slightly different between the selection setups (

Table 1). When the filtering step excluded mutations below 10% frequency, the cyclic-evolved conditions were found to contain more mutations than the mono-evolved conditions ($p = 0.0005162$, t = -4.2419, df = 17.542 via two-tailed t-test), suggesting that the mono-evolved conditions contained many low-frequency mutations, especially the Bs_root_A setup. Only four fixed mutations were present in all 20 lineages, possibly due to the short transfer times used in

the experiment.

Table 1. Mutation type and number

Category	Bs_root_A	Bs_root_T	Bs_root_AT	Bs_root_TA
Pseudogene	0	1	0	0
Non-coding gene*	0	1	0	0
Coding gene	81	91	88	104
Synonymous	15	15	19	19
Non-synonymous	57	58	47	58
Nonsense	0	1	3	6
InDel**	9	17	19	21
Intergenic***	36	13	16	30
Number of mutations	117	106	104	134
Number of mutations (>10%)	50	69	80	92
Fixed mutations	1	0	2	1

Note: There was no overlap between each mutation type. * Non-coding genes include tRNA, ncRNA and repeat region (IS); ** InDel indicates small insertions or deletions in coding gene regions; *** Intergenic refers to all kinds of mutations occurring in intergenic regions.

Although there was no significant difference in the number of mutations between the

evolution conditions, we predicted that populations evolved under cyclic conditions would show greater genetic diversity than mono-evolved populations at the end of the experiment due to the higher complexity and fluctuating nutrient composition caused by the alternating host plants. Therefore, the genotype diversities of endpoint samples were compared between conditions. Indeed, genotype diversity was significantly lower in mono-evolved conditions than in cyclic-evolved conditions (p = 0.01133, t = -2.9044, df = 14.315 via two-tailed t-test), and lowest in the Bs_root_A condition (**Fig. 3**; p = 0.1049, 0.03864 and 0.02767 via two-tailed t-test compared with Bs_root_T, Bs_root_AT and Bs_root_TA, respectively).

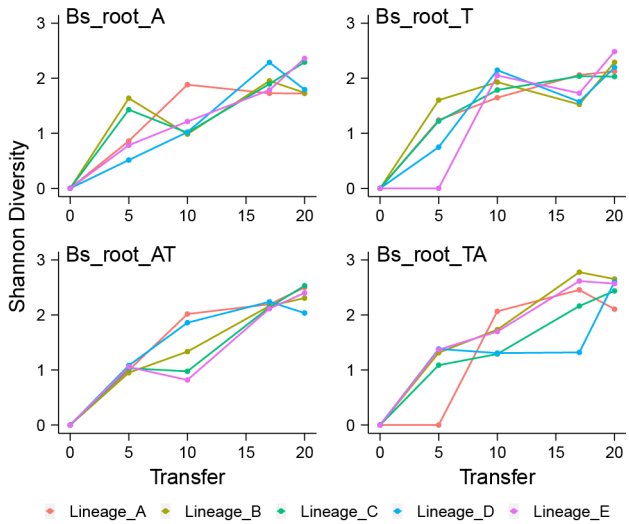

Fig. 3 Genotype diversity. Dynamic distribution of genotype alpha diversity (Shannon method) in each population of four adaptation models over time. Genotypes and their frequencies are from genotype and genealogy analysis using *Lolipop*.

Ecological differentiation and parallel evolution

To infer the ecological differentiation in each lineage and visualise the changes in lineage

frequencies from shared, nested mutation trajectories over time, we utilised the *Lolipop* software package developed by Cooper and colleagues [33, 34]. An average of 16 ± 1.10, 15.6 ± 2.15, 14.6 ± 1.85, and 17.4 ± 2.15 genotypes were obtained in Bs_root_A, Bs_root_T, Bs_root_AT, and Bs_root_TA conditions, respectively, with multiple mutations in each genotype. Consistent with the number of mutations, there were no significant differences in genotype numbers between evolved conditions (Kruskal-Wallis test, $p = 0.3129$). Overall, the number of genotypes continuously increased in all conditions, although it fell in some lineages at certain timepoints, consistently with the detected genotype diversity in each condition. Notably, neither genotype number nor diversity reached a peak within the time frame of the experiment (**Fig. 3**).

Each of the lineages was dominated by a few genotypes containing one or more mutations in certain genes. In general, *sinR*, *pstBA*, *yuxH*, *sigD* and eight flagellum-related genes were the most selected, demonstrating a high parallel evolution at gene and function levels within and between different evolved conditions (**Fig. 4**). Diverse functional genes were mutated, among which bacterial motility-related genes were targeted most frequently, indicating high parallelism at the functional level across all environments. To further compare genetic similarity between conditions, we determined the Jaccard Index (J) of all pairs of lineages within each condition. The Jaccard Index is commonly used for measuring similarity, indicating how likely it is for the same gene to be mutated in two separate lineages [37, 38], ranging from 0 to 1. Again, we observed relatively lower genetic similarity in mono-evolved conditions than in cyclic-evolved conditions, and lowest genetic similarity within the Bs_root_A condition,

significantly lower than in Bs_root_T ($p = 0.0249$, t = -2.4471, df = 17.998 via two-tailed t-test) and the other two cyclic-evolved conditions ($p < 0.001$ and < 0.05, respectively; **Fig. 5**).

Subsequently, we compared the genetic similarity between different evolved conditions. The similarity between the two cyclic-evolved conditions was much higher than the two mono-evolved conditions (p = 2.628e-12, t = -10.022, df = 38.695 via two-tailed t-test), and the similarity between Bs_root_A and two cyclic conditions were also much lower than the similarity between Bs_root_T and two cyclic conditions (**Fig. 5**). These results strongly indicated that the selection pressure imposed by the *A. thaliana* was much weaker than observed with tomato, and the tomato root was potentially the main selective factor in the two cyclic-evolved conditions.

We observed high parallelism from root colonisation ability and morphotype to functional pathway and gene levels, as well as extensive parallelism at the level of individual nucleotides (**Dataset S1**). Strikingly, 18 of 20 lineages contained a frameshift in the *flhB* gene required for flagellum and nanotube assembly [39]. Another 8 bp deletion found in the *yuxH* gene, involved in c-di-GMP regulation in *B. subtilis* [40, 41], was detected in 15 lineages. Additional high parallelism mutations at the nucleotide level, present in more than 10 lineages and belonging to nonsynonymous mutations, occurred in *hag* and *sigD* genes. Notably, all mutations mentioned above reached a high frequency from 12.9% to 68.53% in the evolution conditions. We did not identify these mutations in the ancestor strain stock below a frequency of 5%, but we cannot rule out that they were already acquired in the overnight culture used to start the experimental evolution.

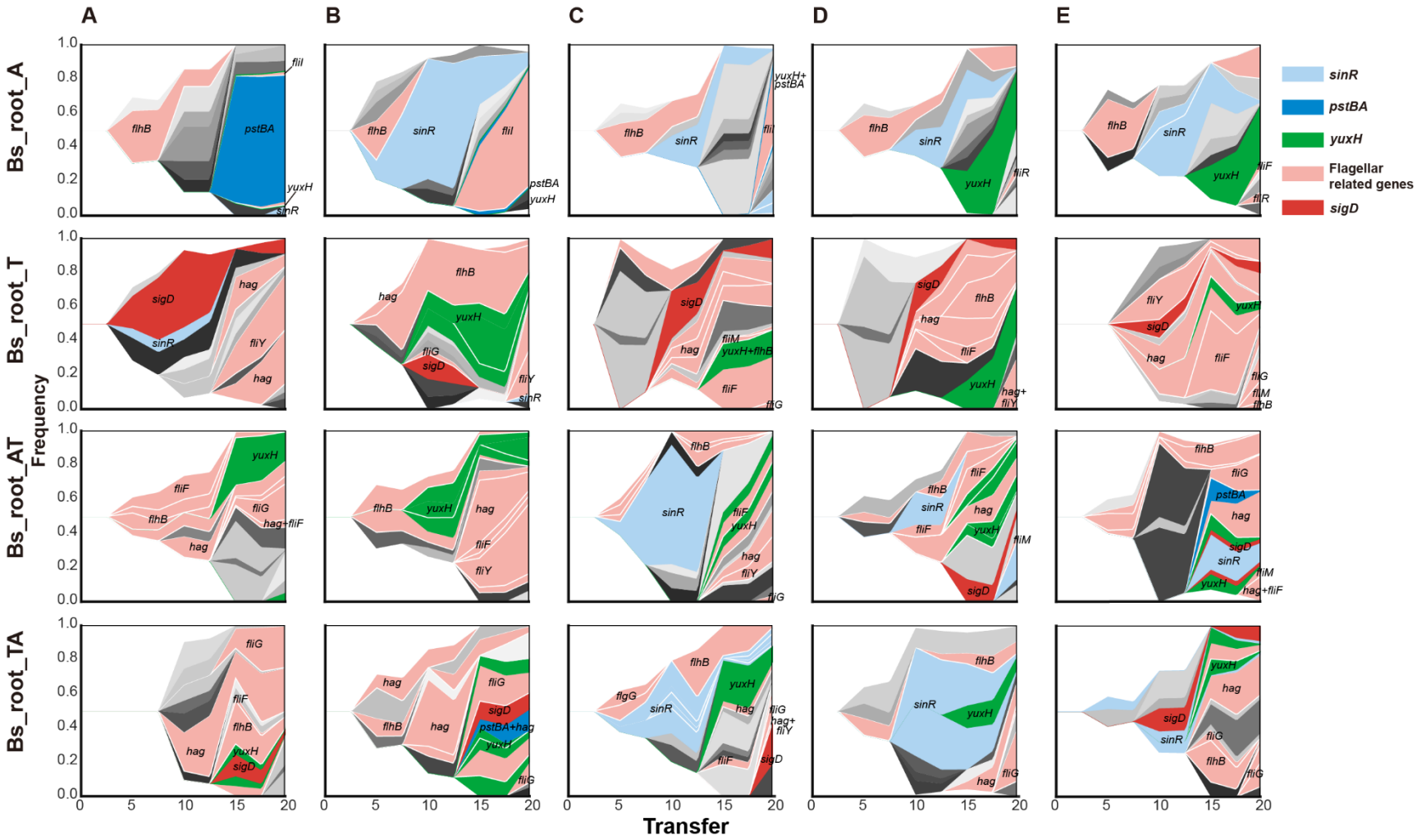

1

2 **Fig. 4 Evolutionary dynamics of *B. subtilis* during plant root colonisation.** Each shade or colour represents a different genotype and vertical

area corresponds to genotype frequency, inferred by *Lolipop*. Genotypes under selective pressure in certain conditions are highlighted in different colours and with annotations within or near shadows, while other genotypes are in different levels of grey without annotation. Nested genotypes of the highlighted genotype are highlighted with the same colour, except for nested genotypes which also contain genes under selective pressure. Notably, some genotypes are less abundant in the figure because their frequencies were similar to their nested genotypes (e.g., *fliI* and *yuxH* in lineage A of Bs_root_A, *pstBA* and *yuxH* in lineage B and C of Bs_root_A). Different colours represent different genotypes containing certain targeted genes, flagellar-related genes including *fliF*, *fliI*, *fliR*, *flhB*, *fliG*, *fliM*, *fliY*, and *hag*. Genotypes containing more than one targeted gene are coloured to match the gene displayed in the front.

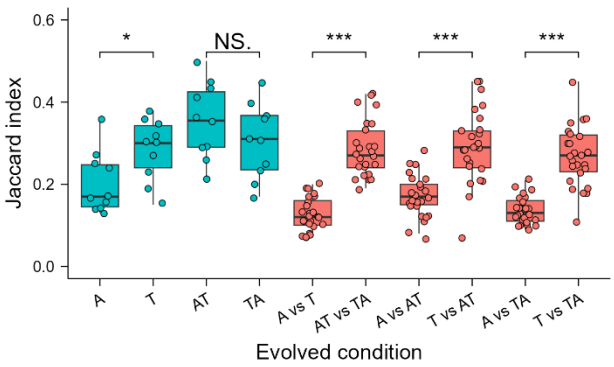

Fig. 5 Parallelism. Degree of parallelism within and between each evolved environment was estimated using the Jaccard index. Asterisks indicate significant differences between different environment combinations (*p <0.05, ***p <0.001, by student's unpaired two-tailed t-test). Boxes indicate Q1−Q3, lines indicate the median, and circles indicate the J value of each pair within (blue) or between (pink) evolved conditions.

B. subtilis adapts specifically towards different plant species

The lower mutation number (frequency >10%), lower genotype diversity, and lower genetic similarity of Bs_root_A strongly imply that the adaptation strategies between Bs_root_A and the other three conditions differed. Therefore, we focused on genes with a mutation frequency >10% and categorised them based on KEGG pathways. Overall, bacterial motility proteins, genetic information processing and metabolism-related genes were mutated more frequently and reached high frequencies, account for 61.36% of mutated genes (frequency >10%).

As mentioned above, bacterial motility proteins were the most selected in our experiment. Among the revealed motility protein genes, eight of eleven were flagellar structure protein-

27 coding genes (**Fig. 6**) [42], and could be categorised into filament-coding genes (flagellin, *hag*),
28 basal body-coding genes (*fliF*, *fliG*, *fliM*, and *fliY*) and flagellar type III secretion (T3S)
29 apparatus protein genes (*fliI*, *fliR*, and *flhB*) [42]. Although bacterial motility genes were
30 targeted frequently in all conditions, *fliI* and *fliR* were only mutated in Bs_root_A, and
31 mutations in *fliG*, *fliY* and *hag* were only absent in Bs_root_A. FliI is a flagellar-specific ATPase
32 functioning in the export of flagellar proteins [43], and FliR is part of the T3S apparatus [44]
33 required for flagellum and nanotube assembly. Another gene required for flagellum and
34 nanotube assembly, *flhB* [39], was mutated in all evolved conditions. FliG is involved directly
35 in flagellar rotation[45], FliY interacts with the chemotaxis system and controls the direction
36 of flagellar rotation [42, 46], and *hag* encodes the flagellin monomer protein Hag, which is also
37 essential for flagellar assembly [47, 48]. The sigma factor-encoding gene *sigD*, which regulates
38 flagella, motility, chemotaxis and autolysis in *B. subtilis* [48–50], was mutated in all except
39 Bs_root_A samples, while *yuxH* (*pdeH*) encoding a phosphodiesterase that degrades c-di-GMP,
40 was mutated in all conditions and relatively high frequencies. c-di-GMP is a second messenger
41 that regulates diverse cellular processes in bacteria, including bacterial motility, biofilm
42 formation, cell-cell signalling and host colonisation [40, 41]. Overall, species-specific and
43 common mutations in both flagellar structural proteins and motility regulator proteins were
44 identified, which were induced by species-specific evolution stress imposed by different plant
45 species and the same static hydroponic setup.

46 Mutations in biofilm development gene *sinR*, encoding a DNA-binding protein that
47 regulates the expression of *epsA-O* and *tapA-sipW-tasA* operons involved in matrix production

48 [51, 52], was only detected transiently with low frequency (maximum 7.19%) in Bs_root_T
49 (**Fig. 4**, **Fig. 6** and **Dataset S2**), while it was observed more frequently and with higher
50 frequency in the other conditions, suggesting an *A. thaliana*-specific mutation.

51 Another suspected *A. thaliana*-specific mutated gene, *pstBA*, encoding a phosphate
52 transport system ATP-binding protein, was only absent in the Bs_root_T sample, and transiently
53 with low frequency in the two cyclic-evolved conditions, but it was detected at high frequency
54 in three of five lineages in Bs_root_A. The *pstBA* gene belongs to the five-gene *pst* operon, and
55 it encodes a member of the PhoP-PhoR two-component signal transduction system [53–55]
56 responsible for phosphate uptake under nutrient stress in *B. subtilis* [55], while the *pst* operon
57 is alkali-inducible [53].

58

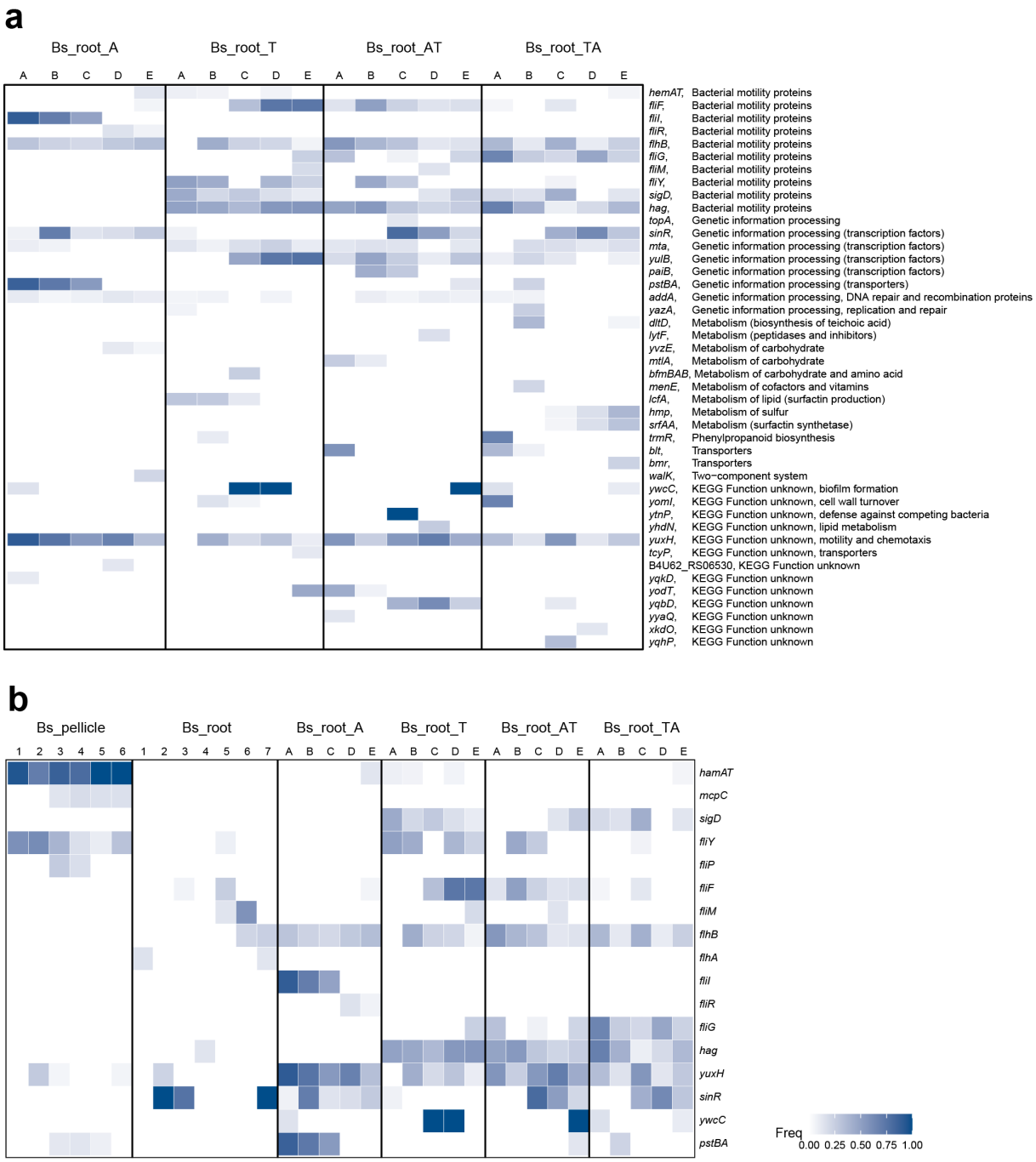

Fig. 6 Parallelism across different experimental setups. (**a**) Genes with mutation frequency >10% in this study. (**b**) Mutated genes shared across different experimental setups. Each column represents one replicate lineage. In each lineage, the colour represents the highest frequency of mutations in that particular gene. Detailed information for these genes and mutations in **(a)** can be found in **Dataset S2**.

65 **DISCUSSION**

66 We explored whether plant-colonising bacteria adapt differently in an alternating host regime
67 compared with the same plant used throughout an experiment, and whether a bacterial species
68 adapts differently to different plant hosts. To do this, experimental evolution and whole-
69 population WGS sequencing were employed to analyse how *B. subtilis* evolves on *A. thaliana*
70 and tomato seedlings, and when these two plant hosts were alternated in a static hydroponic
71 setup [27]. The results did not provide a simple binary answer for the first question, and we
72 observed species-specific adaptation patterns at the genetic level.

73 Similar to several previous studies [23, 24, 27], *B. subtilis* showed rapid improvement in
74 root colonisation ability, albeit at varying rates, as three distinct morphotypes during adaptation
75 in all evolved lineages and conditions. Additionally, the three distinct morphotypes coexisted
76 until the end of the evolution experiment, reaching highly similar ratios in all four evolution
77 experiments. More significantly, complementary effects were observed during root colonisation
78 of *A. thaliana* seedlings through mixing of the three morphotypes from Bs_root_A [27]. Both
79 root colonisation improvement and morphotypic diversification displayed a remarkable degree
80 of parallelism across all evolved conditions. Furthermore, all but one randomly selected isolate
81 from Bs_root_A and Bs_root_T showed impaired swimming and swarming motility.
82 Populations from two host cyclic-evolved conditions shared numerous mutated genes with
83 Bs_root_T, also suggesting similar trade-offs in the alternating plant setup. Analysis of the
84 genetic basis underlying the two levels of parallelism (morphotypes and altered motility)
85 revealed bacterial motility proteins, genetic information processing, and metabolism-related

genes to be mutated more frequently and reaching high frequencies in all evolved conditions. Besides parallelism at phenotypic and functional levels, mutational resemblance was observed in certain genes, even at the individual nucleotide level. Two genes, *flhB* and *yuxH*, showed striking parallelism at both gene and individual nucleotide levels; 18 of 20 lineages contained a frameshift in the *flhB* gene and 15 lineages contained an 8 bp deletion in *yuxH*. The *flhB* gene is required for flagellum and nanotube assembly and *yuxH* is involved in c-di-GMP regulation in *B. subtilis* [40, 41], and both may contribute to adaptation of *B. subtilis* to plant roots by affecting motility. However, reintroduction of single mutations alone or in combination will be necessary in the future to precisely measure the influence of these mutations on fitness. Herein, we identified repeated changes across multiple levels of biological organisation from phenotypic, functional pathways and genes to individual nucleotides [37], demonstrating the overlapping evolutionary patterns employed by *B. subtilis* when adapting to *A. thaliana* and tomato roots, as well as roots in an alternating regime.

The static hydroponic setup used in our study selects for regular root recolonisation by bacterial cells on different plant species, including bacterial traits of chemotaxis, biofilm formation and dispersal [27]. Different histidine kinases influence the phosphorylation level of the global regulator Spo0A [15] when *B. subtilis* forms a biofilm on the roots of *A. thaliana* [16] and tomato [17], and different *Bacillus* species have distinct host plant colonisation abilities [19]. Based on previous results, we hypothesised that *B. subtilis* adaptation to *A. thaliana* or tomato will display distinct gene-level attributes underpinning species-specific adaptation. Although parallelism was identified at phenotypic and nucleotide change levels, obvious

107 differences were detected in the number of mutations (at a frequency >10%), genotype diversity,
108 mutated genes, and genetic similarity between and among different experimental conditions.

109 Fewer mutations (at a frequency >10%), lower genotype diversity and lower within-
110 conditions genetic similarity were observed in mono-evolved conditions, especially in
111 Bs_root_A. The difference between mono-evolved and cyclic-evolved conditions could be
112 explained by a more heterogeneous, multi-resource, spatially-structured environment created
113 by host-cycling, suggesting that environmental heterogeneity might have an important
114 influence on adaptation [34, 37, 56]. When *Pseudomonas fluorescens* was evolved in five
115 different environments varying in terms of resource type and arrangement, more mutations and
116 higher degree of parallelism was observed at the gene level in the most heterogeneous
117 environment [37]. Similarly, evolution of *Pseudomonas aeruginosa* populations on plastic
118 beads that favour a biofilm lifestyle exhibited higher morphologic diversity and mutation rates
119 than planktonic cultures [57]. Consistent with previous studies, the degree of parallel evolution
120 was significantly higher in *B. subtilis* populations evolved in a heterogeneous, multi-resource,
121 spatially-structured environment in the present work.

122 Bs_root_A populations harboured fewest mutations and the least similarity among these,
123 even lower than Bs_root_T samples. Additionally, genetic similarity between the two mono-
124 evolved conditions was much lower than between the two cyclic-evolved conditions, and
125 similarity between Bs_root_A and the two cyclic conditions was also much lower than that
126 between Bs_root_T and the two cyclic conditions. The lowest genetic similarity within
127 Bs_root_A suggests that the fitness landscape in the *A. thaliana* evolving environment might

128 have been more rugged than in tomato [58]. Furthermore, several specific mutated genes were
129 also observed, which were present or absent exclusively in one plant species. These results
130 imply that the adaptation patterns of *B. subtilis* to roots of *A. thaliana* and tomato differed, and
131 *A. thaliana* exerted less influence on the adaptation process in the two cyclic-evolved conditions.
132 A potential key difference between *A. thaliana* and tomato that might alter bacterial evolution
133 is the composition and amount of exudates. In our experimental system, *B. subtilis* was evolved
134 in minimal salt medium (MSM; see **Materials and Methods**), in which bacterial cells are
135 dependent on carbon sources provided by the plant for their growth. The composition and
136 amount of exudates in *A. thaliana* [59] and tomato [60] vary depending on growth stage.

137 We found that the most targeted genes were related to motility, while all lineages displayed
138 improved root colonisation. Motility and biofilm formation are considered to be inversely
139 regulated lifestyles during which bacteria express genes necessary for either motility or biofilm
140 matrix production, but not both simultaneously [61, 62]. Motility is vital for many bacteria, as
141 this process enables them to explore resources and supports the dispersal of progeny [63].
142 Motility is important for the effective root colonisation of different plant species by *B subtilis*
143 under different conditions [18–21]. It is not surprising that the loss of motility is repeatedly
144 evolved in populations growing in well-mixed liquid media where motility is not essential [37],
145 and where the production of proteins for motility, primarily for flagella, is costly in terms of
146 energy and resources [64]. A biofilm-motility trade-off has been suggested for *B. subtilis*
147 evolved on *A. thaliana* roots under shaking conditions [24]. Surprisingly, all mutations in
148 flagellar structure protein-coding genes were nonsynonymous SNPs or InDels, suggesting these

149 mutations may cause loss-of-function of flagella. Notably, a 78 bp duplication (23 amino acids,
150 residues 133−155) occurred in *hag* in three evolved conditions (12 lineages) and reached a high
151 frequency, which would strongly affect the structure and function of flagellin, and therefore cell
152 motility. Additionally, widespread and high-frequency mutations in *sinR* encoding a biofilm
153 master regulator [65], *sigD* encoding sigma factor D [48–50] which regulates flagella, motility,
154 chemotaxis and autolysis of *B. subtilis*, *yuxH* which is involved in c-di-GMP regulation in *B.*
155 *subtilis* [40, 41], and *pstBA* which is responsible for phosphate uptake under nutrient stress in
156 *B. subtilis* [55], were all predicted to regulate the motility-biofilm balance in *B. subtilis*,
157 indicating that pleiotropy is widespread and can influence the adaptation of *B. subtilis*.

158 Finally, we compared the genetic similarities and differences in specific biological
159 functions including aerotaxis, chemotaxis, motility (regulation) and biofilm development, when
160 *B. subtilis* was evolved under different experimental conditions, including a static air-medium
161 pellicle biofilm transfer mode (Bs_pellicle) [66], an *A. thaliana* root colonisation study under a
162 shaking hydroponic setup (Bs_root) [24], and plant root colonisation under a static hydroponic
163 setup (Bs_root_ATTA; **Fig. 6b**). Both common and condition-specific genes were found to
164 carry mutations. We found that *hemAT* was mutated in both Bs_pellicle and Bs_root_ATTA
165 systems, although less frequently in Bs_root_ATTA. Importantly, both experiments were
166 performed under static conditions, where an oxygen gradient is generated in the culture, and
167 HemAT is a key oxygen sensor important during pellicle formation [50]. The lower frequency
168 of mutation in *hemAT* detected in Bs_root_ATTA suggests lower selection for aerotaxis in cells
169 that colonise the submerged parts of plant roots compared with cells localised at the medium-

170 air interface. Interestingly, the sigma factor-encoding gene *sigD* was mutated only in conditions
171 with tomato serving as host in Bs_root_ATTA, suggesting that it is a tomato-specific mutational
172 target gene. Flagella-related genes were found to be mutated in all three conditions, although
173 mutations were detected in different genes and with different frequencies. Furthermore, the c-
174 di-GMP-degrading phosphodiesterase-encoding *pdeH* was mutated in all three conditions, and
175 more frequently in Bs_root_ATTA. The c-di-GMP second messenger modulates diverse cellular
176 activities in bacteria including bacterial motility, biofilm formation, cell-cell signalling and host
177 colonisation [40, 41]. However, previous studies on c-di-GMP signalling have mostly focused
178 on Gram-negative bacteria. The *sinR* gene appears to be a target in plant-specific conditions
179 because it lacked mutations only in Bs_pellicle samples. Another possible static condition-
180 specific target similar to *hemAT* is *pstBA*, which is involved in high-affinity phosphate uptake
181 in *B. subtilis* [55].

182 In conclusion, our study revealed parallel evolution across multiple levels of biological
183 organisation from phenotypic to individual nucleotide levels, while the degree of parallel
184 evolution at the gene level was significantly higher in populations evolved in a heterogeneous,
185 multi-resource, spatially-structured environment. We also observed species-specific adaptation
186 at the genetic level, possibly caused by selection stress imposed by different host plants.
187 Additionally, a strong trade-off between motility and growth as well as biofilm formation was
188 observed under the static selection conditions applied herein. Finally, we identified several
189 condition-specific and common mutated genes by comparing genetic similarities and
190 differences between three studies.

Funding information

This project was supported by the China National GeneBank (CNGB), the Danish National Research Foundation (DNRF137) for the Center for Microbial Secondary Metabolites, and Novo Nordisk Foundation within the INTERACT project of the Collaborative Crop Resiliency Program (NNF19SA0059360).

Conflicts of interest

The authors declare that there are no conflicts of interest.

References

1. **Guo X, Chen F, Gao F, Li L, Liu K, *et al.*** CNSA: A data repository for archiving omics data. *Database* 2020;2020:baaa055.

2. **Chen FZ, You LJ, Yang F, Wang LN, Guo XQ, *et al.*** CNGBdb: China National GeneBank DataBase. *Hereditas* 2020;42:799–809.

3. **Schmidt JE, Bowles TM, Gaudin ACM**. Using ancient traits to convert soil health into crop yield: Impact of selection on maize root and rhizosphere function. *Front Plant Sci* 2016;7:373.

4. **Haichar F el Z, Heulin T, Guyonnet JP, Achouak W**. Stable isotope probing of carbon flow in the plant holobiont. *Curr Opin Biotechnol* 2016;41:9–13.

5. **Venturi V, Keel C**. Signaling in the Rhizosphere. *Trends Plant Sci* 2016;21:187–198.

6. **Sasse J, Martinoia E, Northen T**. Feed Your Friends: Do Plant Exudates Shape the Root Microbiome? *Trends Plant Sci* 2018;23:25–41.

7. **Lareen A, Burton F, Schäfer P**. Plant root-microbe communication in shaping root microbiomes. *Plant Mol Biol* 2016;90:575–587.

8. **Vives-Peris V, de Ollas C, Gómez-Cadenas A, Pérez-Clemente RM**. Root exudates: from plant to rhizosphere and beyond. *Plant Cell Rep* 2020;39:3–17.

9. **Arnaouteli S, Bamford NC, Stanley-Wall NR, Kovács ÁT**. *Bacillus subtilis* biofilm formation and social interactions. *Nat Rev Microbiol* 2021;19:600–614.

10. **Blake C, Christensen MN, Kovács ÁT**. Molecular Aspects of Plant Growth Promotion and Protection by *Bacillus subtilis*. *Molecular Plant-Microbe Interactions* 2021;34:15–25.

11. **Peng G, Mcgregor L, Lahlali R, Gossen BD, Hwang SF, *et al.*** Potential biological control of clubroot on canola and crucifer vegetable crops. *Plant Pathol* 2011;60:566–574.

12. **Wei F, Hu X, Xu X**. Dispersal of Bacillus subtilis and its effect on strawberry phyllosphere microbiota under open field and protection conditions. *Scientific Reports 2016 6:1* 2016;6:1–9.

228 13. **Badri D v., Weir TL, van der Lelie D, Vivanco JM**. Rhizosphere chemical
229 dialogues: plant–microbe interactions. *Curr Opin Biotechnol* 2009;20:642–650.

230 14. **Hamon MA, Lazazzera BA**. The sporulation transcription factor Spo0A is
231 required for biofilm development in *Bacillus subtilis*. *Mol Microbiol*
232 2001;42:1199–1209.

233 15. **Jiang M, Shao W, Perego M, Hoch JA**. Multiple histidine kinases regulate entry
234 into stationary phase and sporulation in Bacillus subtilis. *Mol Microbiol*
235 2000;38:535–542.

236 16. **Chen Y, Cao S, Chai Y, Clardy J, Kolter R, *et al.*** A *Bacillus subtilis* sensor
237 kinase involved in triggering biofilm formation on the roots of tomato plants. *Mol*
238 *Microbiol* 2012;85:418–430.

239 17. **Beauregard PB, Chai Y, Vlamakis H, Losick R, Kolter R**. Bacillus subtilis
240 biofilm induction by plant polysaccharides. *Proc Natl Acad Sci U S A*
241 2013;110:1621–1630.

242 18. **Tian T, Sun B, Shi H, Gao T, He Y, *et al.*** Sucrose triggers a novel signaling
243 cascade promoting Bacillus subtilis rhizosphere colonization. *ISME J*
244 2021;15:2723–2737.

245 19. **Zhang N, Wang D, Liu Y, Li S, Shen Q, *et al.*** Effects of different plant root
246 exudates and their organic acid components on chemotaxis, biofilm formation and
247 colonization by beneficial rhizosphere-associated bacterial strains. *Plant Soil*
248 2014;374:689–700.

249 20. **Gao S, Wu H, Yu X, Qian L, Gao X**. Swarming motility plays the major role in
250 migration during tomato root colonization by Bacillus subtilis SWR01. *Biological*
251 *Control* 2016;98:11–17.

252 21. **Allard-Massicotte R, Tessier L, Lécuyer F, Lakshmanan V, Lucier JF, *et al.***
253 *Bacillus subtilis* Early Colonization of *Arabidopsis thaliana* Roots involves
254 multiple chemotaxis receptors. *mBio* 2016;7:e01664-16.

255 22. **Lenski RE**. What is adaptation by natural selection? Perspectives of an
256 experimental microbiologist. *PLoS Genet* 2017;13:e1006668.

257 23. **Lin Y, Alstrup M, Pang JKY, Maróti G, Er-Rafik M, *et al.*** Adaptation of

258 *Bacillus thuringiensis* to Plant Colonization Affects Differentiation and Toxicity.
259 *mSystems* 2021;6:e00864-21.

260 24. **Nordgaard M, Blake C, Maróti G, Hu G, Wang Y, *et al.*** Experimental evolution
261 of *Bacillus subtilis* on *Arabidopsis thaliana* roots reveals fast adaptation and
262 improved root colonization. *iScience* 2022;25:104406.

263 25. **Li E, Zhang H, Jiang H, Pieterse CMJ, Jousset A, *et al.*** Experimental-
264 evolution-driven identification of arabidopsis rhizosphere competence genes in
265 pseudomonas protegens. *mBio* 2021;12:e00927-21.

266 26. **Li M, Guo J, Ren T, Luo G, Shen Q, *et al.*** Crop rotation history constrains soil
267 biodiversity and multifunctionality relationships. *Agric Ecosyst Environ*
268 2021;319:107550.

269 27. **Blake C, Nordgaard M, Maróti G, Kovács ÁT**. Diversification of *Bacillus*
270 *subtilis* during experimental evolution on *Arabidopsis thaliana* and the
271 complementarity in root colonization of evolved subpopulations. *Environ*
272 *Microbiol* 2021;23:6122–6136.

273 28. **Chen A, Liao S, Cheng M, Ma K, Wu L, *et al.*** Spatiotemporal transcriptomic
274 atlas of mouse organogenesis using DNA nanoball-patterned arrays. *Cell*
275 2022;185:1777-1792.e21.

276 29. **Han L, Wei X, Liu C, Volpe G, Zhuang Z, *et al.*** Cell transcriptomic atlas of the
277 non-human primate *Macaca fascicularis*. *Nature* 2022;604:723–731.

278 30. **Chen Y, Chen Y, Shi C, Huang Z, Zhang Y, *et al.*** SOAPnuke: A MapReduce
279 acceleration-supported software for integrated quality control and preprocessing
280 of high-throughput sequencing data. *Gigascience* 2018;7:gix120.

281 31. **Deatherage DE, Barrick JE**. Identification of Mutations in Laboratory-Evolved
282 Microbes from Next-Generation Sequencing Data Using breseq. *Methods Mol*
283 *Biol* 2014;1151:165–188.

284 32. **Barrick JE, Colburn G, Deatherage DE, Traverse CC, Strand MD, *et al.***
285 Identifying structural variation in haploid microbial genomes from short-read
286 resequencing data using breseq. *BMC Genomics* 2014;15:1039.

287 33. **Scribner MR, Santos-Lopez A, Marshall CW, Deitrick C, Coopera VS, *et al.***

288 Parallel evolution of tobramycin resistance across species and environments.
289 *mBio* 2020;11:e00932-20.

290 34. **Harris KB, Flynn KM, Cooper VS**. Polygenic Adaptation and Clonal
291 Interference Enable Sustained Diversity in Experimental *Pseudomonas*
292 *aeruginosa* Populations. *Mol Biol Evol* 2021;38:5359–5375.

293 35. **Kovács ÁT, Grau R, Pollitt EJG**. Surfing of bacterial droplets: Bacillus subtilis
294 sliding revisited. *Proceedings of the National Academy of Sciences*
295 2017;114:E8802.

296 36. **Hölscher T, Kovács ÁT**. Sliding on the surface: bacterial spreading without an
297 active motor. *Environ Microbiol* 2017;19:2537–2545.

298 37. **Bailey SF, Rodrigue N, Kassen R**. The Effect of Selection Environment on the
299 Probability of Parallel Evolution. *Mol Biol Evol* 2015;32:1436–1448.

300 38. **Bailey SF, Blanquart F, Bataillon T, Kassen R**. What drives parallel evolution?:
301 How population size and mutational variation contribute to repeated evolution.
302 *BioEssays* 2017;39:1600176.

303 39. **Kuhlen L, Johnson S, Zeitler A, Bäurle S, Deme JC, *et al.*** The substrate
304 specificity switch FlhB assembles onto the export gate to regulate type three
305 secretion. *Nat Commun* 2020;11:1296.

306 40. **Chen Y, Chai Y, Guo J-H, Losick R**. Evidence for Cyclic Di-GMP-Mediated
307 Signaling in Bacillus subtilis. *J Bacteriol* 2012;194:5080–5090.

308 41. **Gao X, Mukherjee S, Matthews PM, Hammad LA, Kearns DB, *et al.***
309 Functional Characterization of Core Components of the Bacillus subtilis Cyclic-
310 Di-GMP Signaling Pathway. *J Bacteriol* 2013;195:4782–4792.

311 42. **Mukherjee S, Kearns DB**. The structure and regulation of flagella in *Bacillus*
312 *subtilis*. *Annu Rev Genet* 2014;48:319–340.

313 43. **Ibuki T, Imada K, Minamino T, Kato T, Miyata T, *et al.*** Common architecture
314 of the flagellar type III protein export apparatus and F- and V-type ATPases. *Nat*
315 *Struct Mol Biol* 2011;18:277–282.

316 44. **Kuhlen L, Abrusci P, Johnson S, Gault J, Deme J, *et al.*** Structure of the Core
317 of the Type Three Secretion System Export Apparatus. *Nat Struct Mol Biol*

318 2018;25:583.

319 45. **Ward E, Kim EA, Panushka J, Botelho T, Meyer T, *et al.*** Organization of the
320 flagellar switch complex of Bacillus subtilis. *J Bacteriol* 2019;201:e00626-18.

321 46. **Sircar R, Greenswag AR, Bilwes AM, Gonzalez-Bonet G, Crane BR**. Structure
322 and activity of the flagellar rotor protein FliY: A member of the CheC phosphatase
323 family. *Journal of Biological Chemistry* 2013;288:13493–13502.

324 47. **LaVallie ER, Stahl ML**. Cloning of the flagellin gene from Bacillus subtilis and
325 complementation studies of an in vitro-derived deletion mutation. *J Bacteriol*
326 1989;171:3085–3094.

327 48. **Hölscher T, Schiklang T, Dragoš A, Dietel AK, Kost C, *et al.*** Impaired
328 competence in flagellar mutants of Bacillus subtilis is connected to the regulatory
329 network governed by DegU. *Environ Microbiol Rep* 2018;10:23–32.

330 49. **Marquez LM, Helmann JD, Ferrari E, Parker HM, Ordal GW, *et al.*** Studies
331 of σ^D-dependent functions in *Bacillus subtilis*. *J Bacteriol* 1990;172:3435–3443.

332 50. **Hölscher T, Bartels B, Lin YC, Gallegos-Monterrosa R, Price-Whelan A, *et*
333 *al.*** Motility, Chemotaxis and Aerotaxis Contribute to Competitiveness during
334 Bacterial Pellicle Biofilm Development. *J Mol Biol* 2015;427:3695–3708.

335 51. **Kearns DB**. A field guide to bacterial swarming motility. *Nature Reviews*
336 *Microbiology* 2010;8:634–644.

337 52. **Chu F, Kearns DB, Branda SS, Kolter R, Losick R**. Targets of the master
338 regulator of biofilm formation in Bacillus subtilis. *Mol Microbiol* 2006;59:1216–
339 1228.

340 53. **Atalla A, Schumann W**. The *pst* Operon of *Bacillus subtilis* Is Specifically
341 Induced by Alkali Stress. *J Bacteriol* 2003;185:5019–5022.

342 54. **Allenby NEE, O'Connor N, Prágai Z, Carter NM, Miethke M, *et al.*** Post-
343 transcriptional regulation of the *Bacillus subtilis pst operon* encoding a phosphate-
344 specific ABC transporter. *Microbiology (N Y)* 2004;150:2619–2628.

345 55. **Moreno-Letelier A, Olmedo G, Eguiarte LE, Martinez-Castilla L, Souza V**.
346 Parallel Evolution and Horizontal Gene Transfer of the *pst* Operon in Firmicutes
347 from Oligotrophic Environments. *Int J Evol Biol* 2011;2011:781642.

348 56. **Bram Van den Bergh, Toon Swings, Maarten Fauvart JM**. Experimental
349 Design, Population Dynamics, and Diversity in Microbial Experimental Evolution.
350 *Microbiology and Molecular Biology Reviews* 2018;82:e00008-18.

351 57. **Flynn KM, Dowell G, Johnson TM, Koestler BJ, Waters CM, *et al.*** Evolution
352 of ecological diversity in biofilms of Pseudomonas aeruginosa by altered cyclic
353 diguanylate signaling. *J Bacteriol* 2016;198:2608–2618.

354 58. **Ferretti L, Weinreich D, Tajima F, Achaz G**. Evolutionary constraints in fitness
355 landscapes. *Heredity 2018 121:5* 2018;121:466–481.

356 59. **Chaparro JM, Badri D V, Bakker MG, Sugiyama A, Manter DK, *et al.*** Root
357 Exudation of Phytochemicals in Arabidopsis Follows Specific Patterns That Are
358 Developmentally Programmed and Correlate with Soil Microbial Functions. *PLoS*
359 *One* 2013;8:e55731.

360 60. **Kravchenko L V., Azarova TS, Leonova-Erko EI, Shaposhnikov AI,**
361 **Makarova NM, *et al.*** Root exudates of tomato plants and their effect on the
362 growth and antifungal activity of Pseudomonas strains. *Microbiology (N Y)*
363 2003;72:37–41.

364 61. **Guttenplan SB, Kearns DB**. Regulation of flagellar motility during biofilm
365 formation. *FEMS Microbiol Rev* 2013;37:849–871.

366 62. **van Ditmarsch D, Boyle KE, Sakhtah H, Oyler JE, Nadell CD, *et al.***
367 Convergent evolution of hyperswarming leads to impaired biofilm formation in
368 pathogenic bacteria. *Cell Rep* 2013;4:697–708.

369 63. **Wadhwa N, Berg HC**. Bacterial motility: machinery and mechanisms. *Nat Rev*
370 *Microbiol* 2022;20:161–173.

371 64. **Keegstra JM, Carrara F, Stocker R**. The ecological roles of bacterial
372 chemotaxis. *Nat Rev Microbiol* 2022;20:491–504.

373 65. **Kearns DB, Chu F, Branda SS, Kolter R, Losick R**. A master regulator for
374 biofilm formation by Bacillus subtilis. *Mol Microbiol* 2005;55:739–749.

375 66. **Dragoš A, Lakshmanan N, Martin M, Horváth B, Maróti G, *et al.*** Evolution
376 of exploitative interactions during diversification in *Bacillus subtilis* biofilms.
377 *FEMS Microbiol Ecol* 2018;94:fix155.